Proceedings of the
47th IEEE Conference on Decision and Control
Cancun, Mexico, Dec. 9-11, 2008

A State Predictor for Bilateral Teleoperation with Communication Time Delay

Kouei Yoshida, Toru Namerikawa and Oliver Sawodny

Abstract— **In this paper, the new state predictors are proposed to improve the performance of the predictors in predictive controller for teleoperation with time delay. The proposed state predictors are designed based on solution trajectories of the dynamics. The prediction errors of the proposed predictors do not depend on past prediction errors. To achieve non-delayed synchronization, proposed predictors are incorporated to the predictive control structure. Using the Lyapunov stability method, the proposed control structure is shown to be stable even in the presence of time delay. Experimental results show the effectiveness of our proposed teleoperation.**

I. Introduction

Teleoperation system can extend a human's reach to a remote site and has been developed and motivated by large variety of applications . It is well known that communication delay may destabilize the system and degrade the closed loop performance. Hence it is necessary to improve the closed loop performance while preserving stability.

There are many control schemes proposed for dealing with the time delay in teleoperation systems [1]. The passivity-based approach [2], [3] guarantee stability by making the communication channel a passive loss-less transmission line. These schemes were extended to provide position tracking performance improvement [4]-[6], stability in time varying delay [7], [8] and stability in 4ch architecture framework [9]. On the other hand, robustness of several controllers was analyzed to deal with the time delay [10]-[12]. However, these method can not avoid delayed position or force tracking and the performance was degradad by the large time delay bacause of low gain and high damping.

To achieve performance improvement or non-delayed position or force tracking, the predictive approach was proposed in [13]-[17]. The control schemes in [13], [14] attempt reduction of the delay effect in master side by predicting information in slave side. These schemes improve the performance but position tracking is delayed bacause the state of master was not predicted. In [15], [16], the predictive control was proposed with master and slave state prediction to attempt non-delayed position and force tracking or realization delay-free system. These method can improve the performance of overall system while preserving closed loop stability. In these approach, the operator and environmental models are required for the control law. Practically, the dynamics of operator and environment are very complicated and it is difficult to obtain accurate model. In [17], the predictive PD control was proposed based on [16]. This method do not require the operator and environmental model. Furthermore, if operator and environmental force change slowly during delay, the prediction error is small and delay-free dynamics is realized. However, the prediction errors in [16] [17] are affected by past prediction errors. Thus, convergence of prediction error to zero requires infinite time.

In this paper, the new state predictors are proposed to improve the performance of predictors in [16] [17]. The proposed state predictors are designed based on solution trajectories of the dynamics. This prediction method is similar to the method in [18], [19]. The prediction errors of the proposed predictors do not depend on past prediction errors. Furthermore, the prediction errors converge to zero in finite time under certain condition. Proposed predictors are incorporated to the control structure which is same as [17]. By using the Lyapunov stability method, the proposed control structure is shown to be stable even in the presence of time delay. Experimental results show the effectiveness of our proposed teleoperation.

II. Problem Formulation

A. Dynamics of Teleoperation System

Assuming absence of friction and other disturbances and compensation of gravity effect, the master and slave robot dynamics with n-DOF are described as

$$\begin{aligned} \boldsymbol{M_m}(\boldsymbol{q_m})\ddot{\boldsymbol{q}}_{\boldsymbol{m}} + \boldsymbol{C_m}(\boldsymbol{q_m}, \dot{\boldsymbol{q}}_{\boldsymbol{m}})\dot{\boldsymbol{q}}_{\boldsymbol{m}} &= \boldsymbol{\tau_m} + \boldsymbol{\tau_{op}} \quad (1)\\ \boldsymbol{M_s}(\boldsymbol{q_s})\ddot{\boldsymbol{q}}_{\boldsymbol{s}} + \boldsymbol{C_s}(\boldsymbol{q_s}, \dot{\boldsymbol{q}}_{\boldsymbol{s}})\dot{\boldsymbol{q}}_{\boldsymbol{s}} &= \boldsymbol{\tau_s} - \boldsymbol{\tau_{env}} \quad (2) \end{aligned}$$

where the "m" and "s" denote the master and the slave indexes respectively, $\boldsymbol{q_m},\ \boldsymbol{q_s} \in R^{n\times 1}$ are the joint angle vectors, $\boldsymbol{\tau_m},\ \boldsymbol{\tau_s} \in R^{n\times 1}$ are the input torque vectors, $\boldsymbol{\tau_{op}} \in R^{n\times 1}$ is the operational torque vectors applied to the master arm by human operator, $\boldsymbol{\tau_{env}} \in R^{n\times 1}$ is the environmental torque vectors applied to environment by the slave arm, $\boldsymbol{M_m}(\boldsymbol{q_m}),\ \boldsymbol{M_s}(\boldsymbol{q_s}) \in R^{n\times n}$ are the symmetric and positive definite inertia matrices, $\boldsymbol{C_m}(\boldsymbol{q_m}, \dot{\boldsymbol{q}}_{\boldsymbol{m}})\dot{\boldsymbol{q}}_{\boldsymbol{m}},\ \boldsymbol{C_s}(\boldsymbol{q_s}, \dot{\boldsymbol{q}}_{\boldsymbol{s}})\dot{\boldsymbol{q}}_{\boldsymbol{s}} \in R^{n\times 1}$ are the centrifugal and Coriolis torque vectors. Since matrices $\boldsymbol{M_m}, \boldsymbol{M_s}, \boldsymbol{C_m}, \boldsymbol{C_s}$ are linear in terms of the parameters [15], we can rewrite

$$\begin{aligned} \boldsymbol{M_m}(\boldsymbol{q_m})\ddot{\boldsymbol{q}}_{\boldsymbol{m}} + \boldsymbol{C_m}(\boldsymbol{q_m}, \dot{\boldsymbol{q}}_{\boldsymbol{m1}})\dot{\boldsymbol{q}}_{\boldsymbol{m2}} &= \boldsymbol{Y_m}(\ddot{\boldsymbol{q}}_{\boldsymbol{m}}, \dot{\boldsymbol{q}}_{\boldsymbol{m1}}, \dot{\boldsymbol{q}}_{\boldsymbol{m2}}, \boldsymbol{q_m})\boldsymbol{\theta_m}\\ \boldsymbol{M_s}(\boldsymbol{q_s})\ddot{\boldsymbol{q}}_{\boldsymbol{s}} + \boldsymbol{C_s}(\boldsymbol{q_s}, \dot{\boldsymbol{q}}_{\boldsymbol{s1}})\dot{\boldsymbol{q}}_{\boldsymbol{s2}} &= \boldsymbol{Y_s}(\ddot{\boldsymbol{q}}_{\boldsymbol{s}}, \dot{\boldsymbol{q}}_{\boldsymbol{s1}}, \dot{\boldsymbol{q}}_{\boldsymbol{s2}}, \boldsymbol{q_s})\boldsymbol{\theta_s} \end{aligned}$$

where $\boldsymbol{Y_m}, \boldsymbol{Y_s} \in R^{n\times m}$ are the regressor matrices, $\boldsymbol{\theta_m}, \boldsymbol{\theta_s} \in R^{m\times 1}$ are the parameter vectors.

K. Yoshida and T. Namerikawa are with Division of Electrical Engineering and Computer Engineering, Graduate School of Natural Science and Technology, Kanazawa University, Kakuma-machi, Kanazawa 920-1192 JAPAN. yoshida@scl.ec.t.kanazawa-u.ac.jp and toru@t.kanazawa-u.ac.jp

O. Sawodny is with the Institute for System Dynamics, Universität Stuttgart, Pfaffenwaldring 9, 70569 Stuttgart, Germany sawodny@isys.uni-stuttgart.de

978-1-4244-3124-3/08/$25.00 ©2008 IEEE

In this paper, the time varying communication delays are considered. It is assumed that the signal transmitted to the slave(master) from master(slave) is delayed as $T_m(t)(T_s(t))$. These delays are assumed to satisfy following assumption.

Assumption 1: The delays $T_m(t), T_s(t)$ can be measured.

Remark 1: Delay estimation has been addressed in the literature in various manners. One of then is the method consists of using time-stamping of the transmitted variable. If the master and slave computers have a synchronized time basis, one-direction time delay can be measured by sending a master/slave time signal t to the slave/master side.

In addition, we assume that the operational torque and environmental torque satisfy the following assumption.

Assumption 2: Let $\tau_{op_j}, \tau_{env_j}$ be j-th element of $\boldsymbol{\tau_{op}}, \boldsymbol{\tau_{env}}$, then, there exist positive constant c_{op_j}, c_{env_j} $(j = 1, \ldots, n)$ such that

$$|\tau_{op_j}(t)| \le c_{op_j} \quad , \quad |\tau_{env_j}(t)| \le c_{env_j}, \forall t, \ (j = 1, \ldots, n) \tag{3}$$

Furthermore, it is assumed that there exist the positive constants $\rho_{op_j}, \rho_{env_j}$ such that

$$\sup_{\theta\in[-T_m(t),0]} |\tau_{op_j}(t+\theta) - \tau_{op_j}(t)| \le \rho_{op_j}, \forall t, \ (j=1, \ldots, n) \tag{4}$$

$$\sup_{\theta\in[-T_s(t),0]} |\tau_{env_j}(t+\theta) - \tau_{env_j}(t)| \le \rho_{env_j}, \forall t, \ (j=1, \ldots, n) \tag{5}$$

B. Control Objectives

The controller will be designed to achieve following objectives.

Control Objective:

1) (Stability) The position errors and the velocity errors are bounded under the communication delay

2) (Non-Delayed Synchronization) If $\boldsymbol{\tau_{op}} = \boldsymbol{\tau_{env}} = 0$, the non-delayed synchronization is achieved as follows

$$\lim_{t\to\infty} \boldsymbol{q_m}(t) - \boldsymbol{q_s}(t) = 0, \quad \lim_{t\to\infty} \dot{\boldsymbol{q}}_{\boldsymbol{m}}(t) - \dot{\boldsymbol{q}}_{\boldsymbol{s}}(t) = 0. \tag{6}$$

3) (Static Force Reflection) If $\ddot{\boldsymbol{q}}_{\boldsymbol{m}} = \ddot{\boldsymbol{q}}_{\boldsymbol{s}} = \dot{\boldsymbol{q}}_{\boldsymbol{m}} = \dot{\boldsymbol{q}}_{\boldsymbol{s}} = 0$, the contact force in slave side are accurately transmitted to the human operator in the master side as $\boldsymbol{\tau_{op}} = \boldsymbol{\tau_{env}}$.

If the control objective 2) is achieved, the position tracking performance degradation due to the delay is alleviated. Note that the control objective 3) means achievement of minimal requirement of transparency [5].

III. Controller Design

This section present the predictor-based control schemes designed to achieve the control objectives. In this paper, a new proposed predictors are incorporated to the control structure which is same as [17]. The control structure is shown in Fig. 1. The proposed controllers consist of three parts, "Predictor", "Trajectory generator" and "Adaptive controller". The blocks of "Trajectory generator" and "Adaptive controller" perform impedance shaping and synchronized control by using the adaptive impedance control framework. The block of "Predictor" predict the master and slave current state in the slave and master side to avoid the use of the delayed information.

A. Impedance Shaping by Adaptive Impedance Control

To transform the control problem of nonlinear dynamics (1)(2) into a control problem of linear systems, we address a linearization by the adaptive impedance control. In the adaptive impedance control framework [20], the reference trajectory is generated based on the target impedance and the adaptive controller drives the robot to follow the generated reference trajectory in order to realize the target impedance.

According to the adaptive impedance control framework, following input torque is given to master and slave.

$$\boldsymbol{\tau_m} = -\boldsymbol{\tau_{op}} + \boldsymbol{Y_m}(\ddot{\boldsymbol{q}}_{\boldsymbol{mr}}, \dot{\boldsymbol{q}}_{\boldsymbol{m}}, \dot{\boldsymbol{q}}_{\boldsymbol{mr}}, \boldsymbol{q_m})\overline{\boldsymbol{\theta}}_{\boldsymbol{m}} - \boldsymbol{K_m}\boldsymbol{r}_m \tag{7}$$

$$\boldsymbol{\tau_s} = \boldsymbol{\tau_{env}} + \boldsymbol{Y_s}(\ddot{\boldsymbol{q}}_{\boldsymbol{sr}}, \dot{\boldsymbol{q}}_{\boldsymbol{s}}, \dot{\boldsymbol{q}}_{\boldsymbol{sr}}, \boldsymbol{q_s})\overline{\boldsymbol{\theta}}_{\boldsymbol{s}} - \boldsymbol{K_s}\boldsymbol{r_s} \tag{8}$$

$$\dot{\overline{\boldsymbol{\theta}}}_{\boldsymbol{i}} = -\boldsymbol{\Gamma_i}\boldsymbol{Y_i^T}(\ddot{\boldsymbol{q}}_{\boldsymbol{ir}}, \dot{\boldsymbol{q}}_{\boldsymbol{i}}, \dot{\boldsymbol{q}}_{\boldsymbol{ir}}, \boldsymbol{q_i})\boldsymbol{r_i}, \ (i = m, s) \tag{9}$$

where $\boldsymbol{e_i} = \boldsymbol{q_i} - \boldsymbol{q_{id}}$, $\dot{\boldsymbol{q}}_{\boldsymbol{ir}} = \dot{\boldsymbol{q}}_{\boldsymbol{id}} - \boldsymbol{\Lambda_i}\boldsymbol{e_i}$, $\boldsymbol{r_i} = \dot{\boldsymbol{e}}_{\boldsymbol{i}} + \boldsymbol{\Lambda_i}\boldsymbol{e_i}(i = m, s)$. $\boldsymbol{\Lambda_m}, \boldsymbol{\Lambda_s}, \boldsymbol{K_m}, \boldsymbol{K_s} \in R^{n\times n}$, $\boldsymbol{\Gamma_m}, \boldsymbol{\Gamma_s} \in R^{m\times m}$ are positive definite matrices, $\overline{\boldsymbol{\theta}} \in R^{m\times 1}$ are the estimated parameter vectors. $\boldsymbol{q_{md}}, \dot{\boldsymbol{q}}_{\boldsymbol{md}}, \ddot{\boldsymbol{q}}_{\boldsymbol{md}}, \boldsymbol{q_{sd}}, \dot{\boldsymbol{q}}_{\boldsymbol{sd}}, \ddot{\boldsymbol{q}}_{\boldsymbol{sd}}$ are the trajectories computed according to following linear equations

$$\begin{aligned} \overline{\boldsymbol{M}}_{\boldsymbol{m}}\ddot{\boldsymbol{q}}_{\boldsymbol{md}} &= \boldsymbol{\tau_{md}} + \boldsymbol{\tau_{op}}, \quad \overline{\boldsymbol{M}}_{\boldsymbol{s}}\ddot{\boldsymbol{q}}_{\boldsymbol{sd}} = \boldsymbol{\tau_{sd}} - \boldsymbol{\tau_{env}} \\ \dot{\boldsymbol{q}}_{\boldsymbol{id}}(0) &= \dot{\boldsymbol{q}}_{\boldsymbol{i}}(0), \ \boldsymbol{q_{id}}(0) = \boldsymbol{q_i}(0) \ \ (i = m, s) \end{aligned} \tag{10}$$

where $\overline{\boldsymbol{M}}_{\boldsymbol{m}} = \mathrm{diag}\{\overline{M}_{m_1}, \ldots, \overline{M}_{m_n}\}$, $\overline{\boldsymbol{M}}_{\boldsymbol{s}} = \mathrm{diag}\{\overline{M}_{s_1}, \ldots, \overline{M}_{s_n}\} \in R^{n\times n}$ are diagonal positive definite matrices, $\boldsymbol{\tau_{md}}, \boldsymbol{\tau_{sd}} \in R^n$ are the new input torque. The computation of $\boldsymbol{q_{md}}, \dot{\boldsymbol{q}}_{\boldsymbol{md}}, \ddot{\boldsymbol{q}}_{\boldsymbol{md}}, \boldsymbol{q_{sd}}, \dot{\boldsymbol{q}}_{\boldsymbol{sd}}, \ddot{\boldsymbol{q}}_{\boldsymbol{sd}}$ are carried out by calculation of $\ddot{\boldsymbol{q}}_{\boldsymbol{md}}$, $\ddot{\boldsymbol{q}}_{\boldsymbol{md}}$ from $\boldsymbol{\tau_{md}} + \boldsymbol{\tau_{op}}$, $\boldsymbol{\tau_{sd}} + \boldsymbol{\tau_{env}}$ at each sampling time and integration of $\ddot{\boldsymbol{q}}_{\boldsymbol{md}}$, $\ddot{\boldsymbol{q}}_{\boldsymbol{sd}}$. Using this control law, the signals $\boldsymbol{e_m}, \dot{\boldsymbol{e}}_{\boldsymbol{m}}, \boldsymbol{e_s}, \dot{\boldsymbol{e}}_{\boldsymbol{s}}$ converge to zero as following lemma.

Lemma 1: [20] Consider the system (1)(2) and control law (7)(8) with the parameter adaptation law (9). Assuming $\boldsymbol{q_{id}}$,$\dot{\boldsymbol{q}}_{\boldsymbol{id}}$,$\ddot{\boldsymbol{q}}_{\boldsymbol{id}}(i = m, s)$ are bounded, then, the origin of $\boldsymbol{e_m}, \dot{\boldsymbol{e}}_{\boldsymbol{m}}, \boldsymbol{e_s}, \dot{\boldsymbol{e}}_{\boldsymbol{s}}$ are asymptotically stable.

From this lemma, the master and slave track to trajectories $\boldsymbol{q_{md}}, \boldsymbol{q_{sd}}$ even in the presence of the parametric uncertainties. Thus, the control problem of nonlinear dynamics (1)(2) have been transformed into a control problem of linear systems (10).

B. Synchronized Control Law with Predicted Value

To achieve the non-delayed synchronization, we consider the synchronized control law with predicted value as follows

$$\boldsymbol{\tau_{md}} = -\overline{\boldsymbol{M}}_{\boldsymbol{m}}\boldsymbol{\Lambda}\dot{\boldsymbol{q}}_{\boldsymbol{md}} + \boldsymbol{K}(\hat{\boldsymbol{r}}_{\boldsymbol{sd}} - \boldsymbol{r_{md}}) \tag{11}$$

$$\boldsymbol{\tau_{sd}} = -\overline{\boldsymbol{M}}_{\boldsymbol{s}}\boldsymbol{\Lambda}\dot{\boldsymbol{q}}_{\boldsymbol{sd}} + \boldsymbol{K}(\hat{\boldsymbol{r}}_{\boldsymbol{md}} - \boldsymbol{r_{sd}}) \tag{12}$$

where, $\boldsymbol{K} = \mathrm{diag}\{K_1, \ldots, K_n\}, \boldsymbol{\Lambda} = \mathrm{diag}\{\lambda_1, \ldots, \lambda_n\} \in R^{n\times n}$ are diagonal positive definite matrices, and $\boldsymbol{r_{md}}, \boldsymbol{r_{sd}}$ are defined as $\boldsymbol{r_{md}} = \dot{\boldsymbol{q}}_{\boldsymbol{md}} + \boldsymbol{\Lambda}\boldsymbol{q_{md}}, \boldsymbol{r_{sd}} = \dot{\boldsymbol{q}}_{\boldsymbol{sd}} + \boldsymbol{\Lambda}\boldsymbol{q_{sd}}$. $\hat{\boldsymbol{r}}_{\boldsymbol{md}}, \hat{\boldsymbol{r}}_{\boldsymbol{sd}}$ are predicted value of $\boldsymbol{r_{md}}, \boldsymbol{r_{sd}}$, output of predictors mentioned in next section. This control law is similar to [4], but including predicted value. Combining the control law (11)(12) with (10) yields

$$\overline{\boldsymbol{M}}_{\boldsymbol{m}}\dot{\boldsymbol{r}}_{\boldsymbol{md}} = \boldsymbol{K}(\hat{\boldsymbol{r}}_{\boldsymbol{sd}} - \boldsymbol{r_{md}}) + \boldsymbol{\tau_{op}} \tag{13}$$

$$\overline{\boldsymbol{M}}_{\boldsymbol{s}}\dot{\boldsymbol{r}}_{\boldsymbol{sd}} = \boldsymbol{K}(\hat{\boldsymbol{r}}_{\boldsymbol{md}} - \boldsymbol{r_{sd}}) - \boldsymbol{\tau_{env}} \tag{14}$$

If $\hat{\boldsymbol{r}}_{\boldsymbol{md}} = \boldsymbol{r_{md}}$ and $\hat{\boldsymbol{r}}_{\boldsymbol{sd}} = \boldsymbol{r_{sd}}$, these equations (13)(14) are equivalent to the dynamics of a teleoperation system in [4] with no delay.

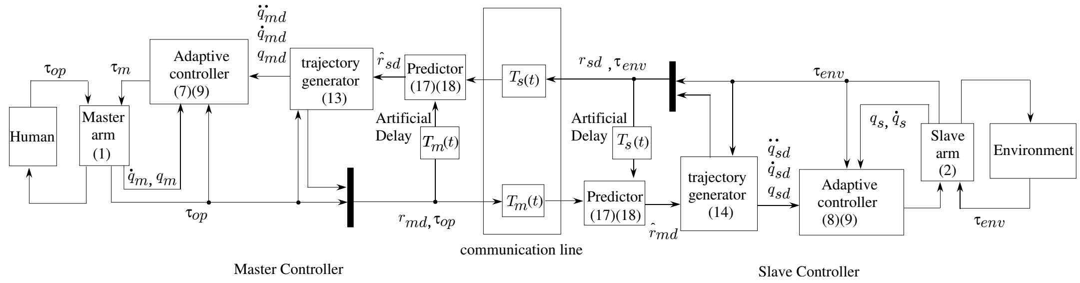

Fig. 1. Control structure of teleoperation

IV. Predictor Design

In this section, we introduce the proposed predictors and compare the performance of proposed predictors with the performance of conventional predictors.

A. Solution Trajectories

A goal of the predictor design is to generate $\hat{\boldsymbol{r}}_{\boldsymbol{sd}}(t)$ at the master side and $\hat{\boldsymbol{r}}_{\boldsymbol{md}}(t)$ at the slave side. The predictions of $\boldsymbol{r_{md}}(t), \boldsymbol{r_{sd}}(t)$ are carried out based on the solution trajectories of (13)(14). Solving the equations (13)(14), the solution trajectories can be given as follows

$$\begin{aligned}\boldsymbol{r_{md}} = &\boldsymbol{e}^{-\overline{\boldsymbol{M}}_{\boldsymbol{m}}^{-1}\boldsymbol{K}T_m(t)}\boldsymbol{r_{md}}(t-T_m(t)) \\ &+\int_{t-T_m(t)}^{t}\boldsymbol{e}^{-\overline{\boldsymbol{M}}_{\boldsymbol{m}}^{-1}\boldsymbol{K}(t-t')}\overline{\boldsymbol{M}}_{\boldsymbol{m}}^{-1}\boldsymbol{K}\hat{\boldsymbol{r}}_{\boldsymbol{sd}}(t')dt' \\ &+\int_{t-T_m(t)}^{t}\boldsymbol{e}^{-\overline{\boldsymbol{M}}_{\boldsymbol{m}}^{-1}\boldsymbol{K}(t-t')}\overline{\boldsymbol{M}}_{\boldsymbol{m}}^{-1}\boldsymbol{\tau_{op}}(t')dt' \end{aligned} \tag{15}$$

$$\begin{aligned}\boldsymbol{r_{sd}} = &\boldsymbol{e}^{-\overline{\boldsymbol{M}}_{\boldsymbol{s}}^{-1}\boldsymbol{K}T_s(t)}\boldsymbol{r_{sd}}(t-T_s(t)) \\ &+\int_{t-T_s(t)}^{t}\boldsymbol{e}^{-\overline{\boldsymbol{M}}_{\boldsymbol{s}}^{-1}\boldsymbol{K}(t-t')}\overline{\boldsymbol{M}}_{\boldsymbol{s}}^{-1}\boldsymbol{K}\hat{\boldsymbol{r}}_{\boldsymbol{md}}(t')dt' \\ &-\int_{t-T_s(t)}^{t}\boldsymbol{e}^{-\overline{\boldsymbol{M}}_{\boldsymbol{s}}^{-1}\boldsymbol{K}(t-t')}\overline{\boldsymbol{M}}_{\boldsymbol{s}}^{-1}\boldsymbol{\tau_{env}}(t')dt'. \end{aligned} \tag{16}$$

We design the predictors by using this solution trajectories. If all terms in right hand of (15)(16) are computable, it is possible to compute $\boldsymbol{r_{md}}(t), \boldsymbol{r_{sd}}(t)$ at current time.

B. Proposed Predictor

At first, we consider the prediction of $\boldsymbol{r_{sd}}(t)$ in the master side. The first term in right hand of (16) is computable in the master side because $\boldsymbol{r_{sd}}(t-T_s(t))$ can be obtained in the master side. And the second term in right hand of (16) is computable in the master side if $\hat{\boldsymbol{r}}_{\boldsymbol{md}}$ is also calculated in the master side. However, the third term in right hand of (16) can not be computable because this computation require the signal $\boldsymbol{\tau_{env}}$ at interval $[t-T_s(t), t]$. Therefore, we use the delayed signal $\boldsymbol{\tau_{env}}(t-T_s(t))$ instead of the signal $\boldsymbol{\tau_{env}}$ at interval $[t-T_s(t), t]$. This idea yields predicted value as follows

$$\begin{aligned}\hat{\boldsymbol{r}}_{\boldsymbol{sd}} = &\boldsymbol{e}^{-\overline{\boldsymbol{M}}_{\boldsymbol{s}}^{-1}\boldsymbol{K}T_s(t)}\boldsymbol{r_{sd}}(t-T_s(t)) \\ &+\int_{t-T_s(t)}^{t}\boldsymbol{e}^{-\overline{\boldsymbol{M}}_{\boldsymbol{s}}^{-1}\boldsymbol{K}(t-t')}\overline{\boldsymbol{M}}_{\boldsymbol{s}}^{-1}\boldsymbol{K}\hat{\boldsymbol{r}}_{\boldsymbol{md}}(t')dt' \\ &+\int_{t-T_s(t)}^{t}\boldsymbol{e}^{-\overline{\boldsymbol{M}}_{\boldsymbol{s}}^{-1}\boldsymbol{K}(t-t')}\overline{\boldsymbol{M}}_{\boldsymbol{s}}^{-1}\boldsymbol{\tau_{env}}(t-T_s(t))dt'. \end{aligned} \tag{17}$$

Furthermore, based on same idea, the prediction of $\boldsymbol{r_{md}}$ is given as

$$\begin{aligned}\hat{\boldsymbol{r}}_{\boldsymbol{md}} = &\boldsymbol{e}^{-\overline{\boldsymbol{M}}_{\boldsymbol{m}}^{-1}\boldsymbol{K}T_m(t)}\boldsymbol{r_{md}}(t-T_m(t)) \\ &+\int_{t-T_m(t)}^{t}\boldsymbol{e}^{-\overline{\boldsymbol{M}}_{\boldsymbol{m}}^{-1}\boldsymbol{K}(t-t')}\overline{\boldsymbol{M}}_{\boldsymbol{m}}^{-1}\boldsymbol{K}\hat{\boldsymbol{r}}_{\boldsymbol{sd}}(t')dt' \\ &+\int_{t-T_m(t)}^{t}\boldsymbol{e}^{-\overline{\boldsymbol{M}}_{\boldsymbol{m}}^{-1}\boldsymbol{K}(t-t')}\overline{\boldsymbol{M}}_{\boldsymbol{m}}^{-1}\boldsymbol{\tau_{op}}(t-T_m(t))dt'. \end{aligned} \tag{18}$$

From this equations, it is obvious that the prediction error converge to zero in finite time if operator and environmental force do not change during the delay time.

C. Boundedness of Prediction Error

The prediction errors $\tilde{\boldsymbol{r}}_{\boldsymbol{md}} = \boldsymbol{r_{md}} - \hat{\boldsymbol{r}}_{\boldsymbol{md}}, \tilde{\boldsymbol{r}}_{\boldsymbol{sd}} = \boldsymbol{r_{sd}} - \hat{\boldsymbol{r}}_{\boldsymbol{sd}}$ are obtained by subtracting (18)(17) from (15)(16).

$$\begin{aligned}\tilde{\boldsymbol{r}}_{\boldsymbol{md}} &= \int_{t-T_m(t)}^{t}\boldsymbol{e}^{-\overline{\boldsymbol{M}}_{\boldsymbol{m}}^{-1}\boldsymbol{K}(t-t')}\overline{\boldsymbol{M}}_{\boldsymbol{m}}^{-1}\{\boldsymbol{\tau_{op}}(t')-\boldsymbol{\tau_{op}}(t-T_m(t))\}dt' \\ \tilde{\boldsymbol{r}}_{\boldsymbol{sd}} &= \int_{t-T_s(t)}^{t}\boldsymbol{e}^{-\overline{\boldsymbol{M}}_{\boldsymbol{s}}^{-1}\boldsymbol{K}(t-t')}\overline{\boldsymbol{M}}_{\boldsymbol{s}}^{-1}\{\boldsymbol{\tau_{env}}(t-T_s(t))-\boldsymbol{\tau_{env}}(t')\}dt' \end{aligned} \tag{19}$$

From these equations, it is clear that the prediction errors are caused by variation of $\boldsymbol{\tau_{op}}, \boldsymbol{\tau_{env}}$ at interval $[t-T_s(t), t], [t-T_m(t), t]$. the prediction errors are bounded as following lemma.

Lemma 2: The prediction errors are bounded as

$$\parallel \tilde{\boldsymbol{r}}_{\boldsymbol{md}}(t) \parallel \leq \sqrt{\sum_{j=1}^{n} c_{m_j}^2}, \left(c_{m_j} = \rho_{op_j}\frac{1-e^{-\overline{M}_{m_j}^{-1}K_jT_m(t)}}{K_j}\right) \tag{20}$$

$$\parallel \tilde{\boldsymbol{r}}_{\boldsymbol{sd}}(t) \parallel \leq \sqrt{\sum_{j=1}^{n} c_{s_j}^2}, \left(c_{s_j} = \rho_{env_j}\frac{1-e^{-\overline{M}_{s_j}^{-1}K_jT_s(t)}}{K_j}\right) \tag{21}$$

where $\parallel \cdot \parallel$ is the Euclidean norm. $c_{m_j}(t), c_{s_j}(t)$ are the bounds of j-th element of $\tilde{\boldsymbol{r}}_{\boldsymbol{md}}, \tilde{\boldsymbol{r}}_{\boldsymbol{sd}}$.

Proof: From the equations (19), the j-th element of $\tilde{\boldsymbol{r}}_{\boldsymbol{md}} = [\tilde{r}_{md_1}, \ldots, \tilde{r}_{md_n}]^T$ is given as follows

$$\tilde{r}_{md_j} = \int_{t-T_m(t)}^{t} e^{-\overline{M}_{m_j}^{-1}K_j(t-t')}\overline{M}_{m_j}^{-1}\{\tau_{op_j}(t')-\tau_{op_j}(t-T_m(t))\}dt'. \tag{22}$$

It is easy to show that the absolute value of (22) satisfies following equation

$$|\tilde{r}_{md_j}| \leq \int_{t-T_m(t)}^{t} e^{-\overline{M}_{m_j}^{-1}K_j(t-t')}\overline{M}_{m_j}^{-1}\Big|\tau_{op_j}(t')-\tau_{op_j}(t-T_m(t))\Big|dt'.$$

Furthermore, *Assumption 2* yield

$$|\tilde{r}_{md_j}| \le \rho_{op_j} \int_{t-T_m(t)}^{t} e^{-\overline{M}_{m_j}^{-1} K_j (t-t')} \overline{M}_{m_j}^{-1} dt' = c_{m_j}.$$

From this inequality, (20) is obtained easily. Similarly, boundedness of $\tilde{\boldsymbol{r}}_{\boldsymbol{sd}}$ can be proven. ■

D. Comparison with Conventional Predictor

If the predictors in [16][17] are used, the prediction errors $\tilde{\boldsymbol{r}}_{\boldsymbol{md}}$ is given as follows

$$\begin{aligned}\tilde{\boldsymbol{r}}_{\boldsymbol{md}} = &\int_{t-T_m(t)}^{t} e^{-\overline{\boldsymbol{M}}_{\boldsymbol{m}}^{-1}\boldsymbol{K}(t-t')} \overline{\boldsymbol{M}}_{\boldsymbol{m}}^{-1} \{\boldsymbol{\tau_{op}}(t') - \boldsymbol{\tau_{op}}(t' - T_m(t))\} dt' \\ &+ e^{-\overline{\boldsymbol{M}}_{\boldsymbol{m}}^{-1}\boldsymbol{K} T_m(t)} \tilde{\boldsymbol{r}}_{\boldsymbol{md}}(t - T_m(t)) \\ &+ \int_{t-T_m(t)}^{t} e^{-\overline{\boldsymbol{M}}_{\boldsymbol{m}}^{-1}\boldsymbol{K}(t-t')} \boldsymbol{E_m} \tilde{\boldsymbol{r}}_{\boldsymbol{m}}(t' - T_m(t)) dt'. \end{aligned} \tag{23}$$

where, $\boldsymbol{E_m}, \boldsymbol{E_s} \in R^{n\times n}$ are gain matrices designed according to procedure given in [16]. The first terms in right hand of (23) are similar to (19). The first terms depend on variation of $\boldsymbol{\tau_{op}}, \boldsymbol{\tau_{env}}$. In addition, the second and third terms in right hand of (23) represent the effect of past prediction errors. From these equations, the convergence of prediction errors require long time even if the first terms become zero. On the other hand, the proposed predictors make prediction errors become zero immediately if the first terms are zero. Same results is given for slave state prediction error.

V. Stability Analysis

In this section, we analyze the master slave position error, velocity error and force reflection. To facilitate the stability analysis, we introduce the error system dynamics. Subtracting (14) from (13), and defining $\boldsymbol{r_{syn}} = \boldsymbol{r_{md}} - \boldsymbol{r_{sd}}$, we have following error system

$$\begin{aligned}\dot{\boldsymbol{r}}_{\boldsymbol{syn}} = &-(\overline{\boldsymbol{M}}_{\boldsymbol{m}}^{-1} + \overline{\boldsymbol{M}}_{\boldsymbol{s}}^{-1})\boldsymbol{K}\boldsymbol{r_{syn}} + \overline{\boldsymbol{M}}_{\boldsymbol{m}}^{-1}\boldsymbol{\tau_{op}} + \overline{\boldsymbol{M}}_{\boldsymbol{s}}^{-1}\boldsymbol{\tau_{env}} \\ &+ \overline{\boldsymbol{M}}_{\boldsymbol{m}}^{-1}\boldsymbol{K}\tilde{\boldsymbol{r}}_{\boldsymbol{sd}} - \overline{\boldsymbol{M}}_{\boldsymbol{s}}^{-1}\boldsymbol{K}\tilde{\boldsymbol{r}}_{\boldsymbol{md}}. \end{aligned} \tag{24}$$

This system (24) is interpreted as stable system affected by the operator and environmental force and prediction errors. The following lemma describes the stability of the system and achievement of the non-delayed synchronization.

Lemma 3: Consider the teleoperation system controlled by proposed controller with *Assumption 1,2*. The following two facts are given.

1) (stability) The position errors and velocity errors are bounded. Furthermore, if $\boldsymbol{r_{syn}}(0) = 0$, the bounds of position errors and velocity errors in steady state ($t \to \infty$) are estimated as follows

$$\| \boldsymbol{q_m} - \boldsymbol{q_s} \| \le \sqrt{\sum_{j=1}^{n} \frac{C_j}{\Lambda_j^2}},\ \| \dot{\boldsymbol{q}}_{\boldsymbol{m}} - \dot{\boldsymbol{q}}_{\boldsymbol{s}} \| \le \sqrt{\sum_{j=1}^{n} 4C_j} \tag{25}$$

where $C_j = \gamma_{op_j}^2 c_{op_j}^2 + \gamma_{env_j}^2 c_{env_j}^2 + \gamma_{m_j}^2 c_{m_j}^2 + \gamma_{s_j}^2 c_{s_j}^2$. $c_{op_j}, c_{env_j}, c_{m_j}, c_{s_j}$ are positive constant defined in *Assumption 2* and *Lemma 2*. $\gamma_{op_j}, \gamma_{env_j}, \gamma_{m_j}, \gamma_{s_j}$ $(j = 1, \dots, n)$ are positive constant such that there exist solution $p_j > 0$ $(j = 1, \dots, n)$ of following LMI given $\gamma_{op_j}, \gamma_{env_j}, \gamma_{m_j}, \gamma_{s_j}$

$$\begin{bmatrix} -2K_j(\overline{M}_{m_j}^{-1} + \overline{M}_{s_j}^{-1})p_j + 1 & p_j\overline{M}_{m_j}^{-1} & p_j\overline{M}_{s_j}^{-1} & p_j\overline{M}_{m_j}^{-1}K_j & p_j\overline{M}_{s_j}^{-1}K_j \\ p_j\overline{M}_{m_j}^{-1} & -\gamma_{op_j}^2 & 0 & 0 & 0 \\ p_j\overline{M}_{s_j}^{-1} & 0 & -\gamma_{env_j}^2 & 0 & 0 \\ p_j\overline{M}_{m_j}^{-1}K_j & 0 & 0 & -\gamma_{m_j}^2 & 0 \\ p_j\overline{M}_{s_j}^{-1}K_j & 0 & 0 & 0 & -\gamma_{s_j}^2 \end{bmatrix} < 0$$

2) (Non-delayed synchronization) If $\boldsymbol{\tau_{op}}, \boldsymbol{\tau_{env}} = 0, \boldsymbol{r_{syn}}(0) \neq 0$, the non-delayed synchronization is achieved as $\lim_{t\to\infty} \| \boldsymbol{q_m} - \boldsymbol{q_s} \|, \| \dot{\boldsymbol{q}}_{\boldsymbol{m}} - \dot{\boldsymbol{q}}_{\boldsymbol{s}} \| = 0$.

Proof: The proof is shown in appendix A. ■

To achieve the *Control Objective 3)*, i.e. force reflection, it is required that the certain condition is satisfied as shown in following lemma.

Lemma 4: If $\ddot{\boldsymbol{q}}_{\boldsymbol{md}} = \ddot{\boldsymbol{q}}_{\boldsymbol{sd}} = \dot{\boldsymbol{q}}_{\boldsymbol{md}} = \dot{\boldsymbol{q}}_{\boldsymbol{sd}} = 0$ and $\tilde{\boldsymbol{r}}_{\boldsymbol{md}}, \tilde{\boldsymbol{r}}_{\boldsymbol{sd}} = 0$ are satisfied, the force reflection $\boldsymbol{\tau_{op}} = \boldsymbol{K}(\boldsymbol{q_{md}} - \boldsymbol{q_{sd}}) = \boldsymbol{\tau_{env}}$ is achieved.

Proof: This lemma is proven by substituting $\ddot{\boldsymbol{q}}_{\boldsymbol{md}} = \ddot{\boldsymbol{q}}_{\boldsymbol{sd}} = \dot{\boldsymbol{q}}_{\boldsymbol{md}} = \dot{\boldsymbol{q}}_{\boldsymbol{sd}} = 0$, $\tilde{\boldsymbol{r}}_{\boldsymbol{md}}, \tilde{\boldsymbol{r}}_{\boldsymbol{sd}} = 0$ for (13)(14). ■

By *Lemma 1*, $\ddot{\boldsymbol{q}}_{\boldsymbol{md}} = \ddot{\boldsymbol{q}}_{\boldsymbol{sd}} = \dot{\boldsymbol{q}}_{\boldsymbol{md}} = \dot{\boldsymbol{q}}_{\boldsymbol{sd}} = 0$ imply that $\ddot{\boldsymbol{q}}_{\boldsymbol{m}} = \ddot{\boldsymbol{q}}_{\boldsymbol{s}} = \dot{\boldsymbol{q}}_{\boldsymbol{m}} = \dot{\boldsymbol{q}}_{\boldsymbol{s}} = 0$ in steady state. Thus, *Control Objective 3)* is achieved if the accelerations and velocities of the robots are zero and prediction errors are zero.

From these lemmas, the achievement of control objectives are concluded as the following theorem.

Theorem 1: Consider the teleoperation system controlled by proposed controller with *Assumption 1,2*. Then, The following three facts are given.

1. The *Control Objective 1)* is achieved.
2. The *Control Objective 2)* is achieved if $\boldsymbol{\tau_{op}}, \boldsymbol{\tau_{env}} = 0$.
3. The *Control Objective 3)* is achieved in steady state if $\ddot{\boldsymbol{q}}_{\boldsymbol{md}} = \ddot{\boldsymbol{q}}_{\boldsymbol{sd}} = \dot{\boldsymbol{q}}_{\boldsymbol{md}} = \dot{\boldsymbol{q}}_{\boldsymbol{sd}} = 0$, $\tilde{\boldsymbol{r}}_{\boldsymbol{md}}, \tilde{\boldsymbol{r}}_{\boldsymbol{sd}} = 0$.

Proof: This theorem can be proven easily from *Lemma 1-4*. ■

Remark 2: In this paper we assume only the boundedness of change of force during delay time for environmental force. Practically, The environmental force depend on slave state. If environmental force depend on slave state, the prediction error depend on slave state. In this case, another analysis is required. It is future work that analysis with this environmental model. The stability for slave hard contact is experimentally evaluated in this paper.

Remark 3: If time delay is large, the operator and environment force change during the delay time may be large and prediction error also increase and tracking error may be very large. Thus, in the large delay case, performance of the controller without prediction may be better than this predictive control.

VI. Simulation

In this section, the performance of the proposed predictors is evaluated by simulation. The proposed predictors are compared with the conventional predictor. we use the model of 2-DOF arm (Fig. 2) for simulation. The design parameters are selected as follows

$$\overline{\boldsymbol{M}}_{\boldsymbol{i}} = \mathrm{diag}(2, 1.5), \boldsymbol{\Lambda} = \mathrm{diag}(2, 1.5), \boldsymbol{K} = \mathrm{diag}(7, 4) \tag{26}$$
$$\boldsymbol{\Gamma_i} = \mathrm{diag}(1, 1, 1), \boldsymbol{K_i} = \mathrm{diag}(8, 5), \boldsymbol{\Lambda_i} = \mathrm{diag}(5, 3), (i = m, s).$$

The gains $\boldsymbol{E_m}, \boldsymbol{E_s} = \mathrm{diag}(-0.2112, -0.2773)$ for conventional predictor are designed according to the procedure in [16]. The delays are $T_m = T_s = 0.5[s]$. The operator torque is shown in Fig. 3 and the environmental torque is zero ($\boldsymbol{\tau_{env}} = 0$). By the definition of $\boldsymbol{\tau_{op}}$, we have

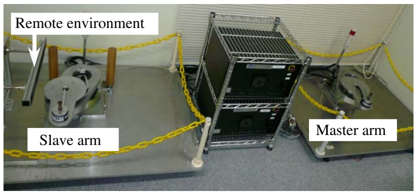

Fig. 2. Experimental setup

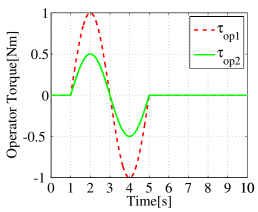

Fig. 3. $\boldsymbol{\tau_{op}}$

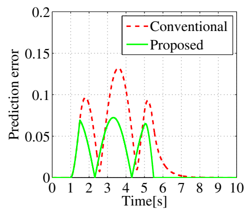

Fig. 4. $\| \tilde{\boldsymbol{r}}_{\boldsymbol{md}} \|$

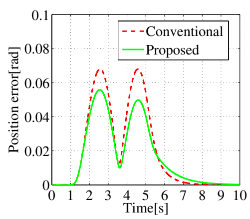

Fig. 5. $\| \boldsymbol{q_m} - \boldsymbol{q_s} \|$

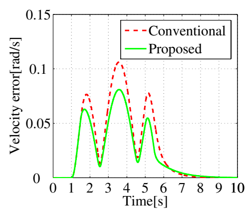

Fig. 6. $\| \dot{\boldsymbol{q}}_{\boldsymbol{m}} - \dot{\boldsymbol{q}}_{\boldsymbol{s}} \|$

$\rho_{op_1} = 0.7654, \rho_{op_2} = 0.3827, \rho_{env_1} = \rho_{env_2} = 0$, $c_{op_1} = 1, c_{op_2} = 0.5, c_{env_1} = c_{env_2} = 0$. From these value and *Lemma 2* and *Lemma 3*, the estimated bounds are given as

$$\| \tilde{\boldsymbol{r}}_{\boldsymbol{md}} \| \leq 0.1146, \ \| \boldsymbol{q_m} - \boldsymbol{q_s} \| \leq 0.0874, \ \| \dot{\boldsymbol{q}}_{\boldsymbol{m}} - \dot{\boldsymbol{q}}_{\boldsymbol{s}} \| \leq 0.3043.$$

Figs. 4, 5 and 6 show the prediction error $\| \tilde{\boldsymbol{r}}_{\boldsymbol{md}} \|$, the position error $\| \boldsymbol{q_m} - \boldsymbol{q_s} \|$ and the velocity error $\| \dot{\boldsymbol{q}}_{\boldsymbol{m}} - \dot{\boldsymbol{q}}_{\boldsymbol{s}} \|$ respectively. As shown these results, the prediction errors, position errors and velocity errors are smaller than the estimated bounds when proposed predictors are used. These errors converge to zero after operator torque become zero. Note that prediction error in proposed predictor case converge to zero quickly because the proposed predictor is independent of past prediction errors. By the equation (19), it is guaranteed that $\| \tilde{\boldsymbol{r}}_{\boldsymbol{md}} \| = 0$ after 5.5[s]. However, when the conventional predictors are used, the convergence of prediction error requires long time.

VII. Experimental Evaluation

In this section, position tracking performance and the performance of the force reflection are evaluated experimentally. The experiments were carried out on a pair of identical 2 degree of freedom robots as shown in Fig. 2. We use DS1104(dSPACE Inc.) as a real-time calculating machine and 1[ms] sampling rate is obtained. All experiments have been done with an artificial time delay as $T_m(t) = T_s(t) = 0.5$[s]. The controller parameters are same as (26). We use the environment of an aluminum wall covered by rubber as shown in Fig. 2. Two cases of experiments are carried out.

- Case 1: The slave moves without any contact
- Case 2: The slave contacts with the environment

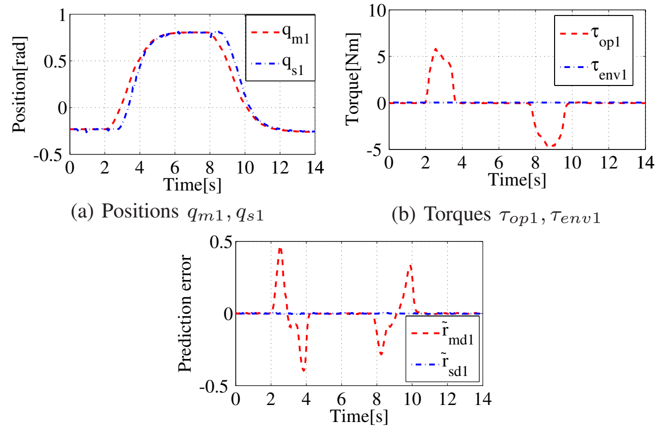

(a) Positions q_{m1}, q_{s1} (b) Torques τ_{op1}, τ_{env1}

(c) Prediction errors $\tilde{r}_{md1}, \tilde{r}_{sd1}$

Fig. 7. Experimental results in free motion (Case 1)

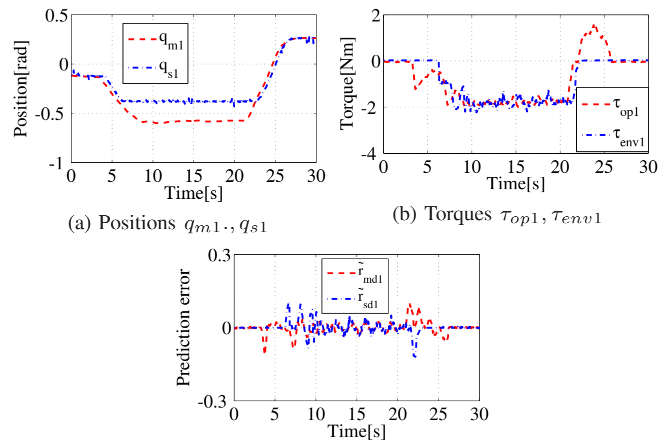

(a) Positions $q_{m1}., q_{s1}$ (b) Torques τ_{op1}, τ_{env1}

(c) Prediction errors $\tilde{r}_{md1}, \tilde{r}_{sd1}$

Fig. 8. Experimental results in constrained motion (Case 2)

Figs. 7(a), (b) and (c) show the joint angles, operator and environmental torques and prediction errors in Case 1 respectively. As shown in these results, the position error is bounded. Furthermore, if $\boldsymbol{\tau_{op}} = \boldsymbol{\tau_{env}} = 0$, non-delayed synchronization is achieved. Compared with the control scheme without prediction [4], the predictive controller attempt non-delayed tracking. The comparison between predictive and non-predictive controller is shown in [17]. Figs. 8(a), (b) and (c) show the results in Case 2. As shown in these results, when slave robot is pushing the environment and the conditions in *Lemma 4* ($\tilde{\boldsymbol{r}}_{\boldsymbol{md}}, \tilde{\boldsymbol{r}}_{\boldsymbol{sd}} = 0$, $\dot{\boldsymbol{q}}_{\boldsymbol{s}} = \dot{\boldsymbol{q}}_{\boldsymbol{m}} = \ddot{\boldsymbol{q}}_{\boldsymbol{s}} = \ddot{\boldsymbol{q}}_{\boldsymbol{m}} = 0$) are satisfied(10[s]-20[s]), the environmental force on contact is accurately transmitted to the operator, i.e., force reflection is achieved.

VIII. Conclusion

In this paper, the new state predictors were proposed to improve the performance of predictors in [16][17]. The prediction errors of the proposed predictors do not depend on past prediction errors. Proposed predictors were incorporated to the control structure which is same as [17] Using the Lyapunov stability method, the proposed control structure was shown to be stable. Simulation and Experimental results showed the effectiveness of our proposed teleoperation.

REFERENCES

[1] P. F. Hokayem and M. W. Spong, "Bilateral teleoperation: An historical survey," *Automatica*, vol. 42, no. 12, pp. 2035-2057, 2006.

[2] R. J. Anderson and M. W. Spong, "Bilateral control of teleoperators with time Delay," *IEEE Trans. Automat. Contr.*, vol. 34, no. 5, pp. 494 - 501, 1989.

[3] G. Niemeyer and J. J. E. Slotine, "Stable adaptive teleoperation " *IEEE J. Oceanic Eng.*, vol. 16, no. 1, pp. 152 - 162, 1991.

[4] N. Chopra and M. W. Spong, "Adaptive synchronization of bilateral teleoperators with time delay," Advances in Telerobotics, springer, pp. 257-270, 2007.

[5] D. Lee and M. W. Spong, "Passive Bilateral Teleoperation with Constant Time Delay," *IEEE Trans. Robot.* , vol.22, no.2, pp. 269-281, 2006.

[6] T. Namerikawa and H. Kawada, "Symmetric Impedance Matched Teleoperation with Position Tracking," in *Proc. Conf. Dec. Contr.*, pp. 4496-4501, 2006.

[7] N. Chopra, M. W. Spong, S. Hirche and M. Buss, "Bilateral teleoperation over the internet,"in *Proc. Amer. Contr. Conf.*, pp. 155-160, 2003.

[8] H. Kawada and T. Namerikawa, "Bilateral Control of Nonlinear Teleoperation with Time Varying Communication Delays," in *Proc. Amer. Contr. Conf.*, pp. 189-194, 2008.

[9] A. Aziminejad, M. Tavakoli, R. V. Patel and M. Moallem, "Transparent time-delayed bilateral teleoperation using wave variables," *IEEE Trans. Contr. Syst. Technol.*, vol. 16, no. 3, pp. 548-555, 2008.

[10] K. Hashtrudi-Zadd, S. E. Salcudean, "Analysis of control architectures for teleoperation systems with impedance/admittance master and slave manipulators," *Int. J. of Robot. res.*, vol.20, no.6, pp 419- 445, 2001.

[11] G.M.H. Leung and B. A. Francis, "Bilateral controller for teleoperators with time delay via μ-Synthesis," *IEEE Trans. Robot. Autom.* , vol. 11, pp 105-116, 2006.

[12] W. -H. Zhu and S. Salcudean, "Stability guaranteed teleoperation: An adaptive motion/force control approach," *IEEE Trans. Autom. Control*, vol.45, no.11, pp. 1951- 1969, 2000.

[13] H. Ching , W.J. Book, "Internet-based bilateral teleoperation based on wave variable with semi-adaptive predictor and direct drift control" J. Dyn. Syst. Measure. Contr., vol. 128, pp. 86-93, 2006.

[14] A. C. Smith and K. Hashtrudi-Zadd, "Adaptive teleoperation using neural network-based predictive control," in *Proc. Conf. Contr. Appl.*, pp. 1269-1274, 2005.

[15] S. Sirouspour, A. Shahdi, "Model predictive control for transparent teleoperation under communication time delay," *IEEE Trans. Robot.* , vol.22, no.6, pp. 1131-1145, 2006.

[16] Y. J. Pan, C. Canudas-de-Wit and O. Sename, "A new predictive approach for bilateral teleoperation with applications to drive-by-wire systems," *IEEE Trans. Robot.* , vol.10, no.6, pp. 1146-1162, 2006.

[17] K. Yoshida, T. Namerikawa, "Predictive PD Control for Teleoperation with Communication Time Delay," in *Proc. 17th IFAC World Congr.*, pp. 12703-12708, 2008.

[18] Z. Artstein, "Linear systems with delayed controls: A reduction, " *IEEE Trans. Autom. Control*, vol.27, no.4, pp. 869- 879, 1982.

[19] E. Witrant, D. Georges, C. Canudas-De-Wit, M. Alamir, "On the use of state predictors in networked control systems, " Lecture Notes in Control and Information Sciences vol. 352, pp. 17-35, 2007

[20] W. S. Lu and Q. H. Meng, "Impedance Control with Adaptation," *IEEE Trans. Robot. Autom.*, Vol.7, No.3, pp. 408-415, 1991.

APPENDIX

A. Proof of Lemma 3

Proof: (proof of 1)) Let q_{m_j}, q_{s_j} be j-th element of the vector $\boldsymbol{q_m}, \boldsymbol{q_s}$. Considering following equation

$$\begin{aligned}|q_{m_j} - q_{s_j}| &= |q_{m_j} - q_{md_j} + q_{md_j} - q_{sd_j} + q_{sd_j} - q_{s_j}| \\ &\le |q_{m_j} - q_{md_j}| + |q_{md_j} - q_{sd_j}| + |q_{sd_j} - q_{s_j}|, \\ |\dot q_{m_j} - \dot q_{s_j}| &= |\dot q_{m_j} - \dot q_{md_j} + \dot q_{md_j} - \dot q_{sd_j} + \dot q_{sd_j} - \dot q_{s_j}| \\ &\le |\dot q_{m_j} - \dot q_{md_j}| + |\dot q_{md_j} - \dot q_{sd_j}| + |\dot q_{sd_j} - \dot q_{s_j}|.\end{aligned}$$

The first and third terms in right hand of above equations are converge to zero in steady state from *Lemma 1*. Therefore we consider the second terms in right hand of above equations. Using the fact that $\overline{\boldsymbol{M}}_{\boldsymbol{m}}, \overline{\boldsymbol{M}}_{\boldsymbol{s}}, \boldsymbol{K}$ are diagonal, the j-th element of equation (24) is given as follows

$$\begin{aligned}\dot r_{syn_j} = &-(\overline{M}_{m_j}^{-1} + \overline{M}_{s_j}^{-1})K_j r_{syn_j} + \overline{M}_{m_j}^{-1}\tau_{op_j} + \overline{M}_{s_j}^{-1}\tau_{env_j} \\ &+ \overline{M}_{m_j}^{-1}K_j\tilde r_{sdj} - \overline{M}_{s_j}^{-1}K_j\tilde r_{mdj} \qquad (27)\end{aligned}$$

where r_{syn_j} is defined as j-th element of $\boldsymbol{r_{syn}}$. Define the Lyapunov candidate $V_j = r_{syn_j} p_j r_{syn_j}$. The derivative of V_j along the solution of the error system gives

$$\begin{aligned}\dot V_j &= -r_{syn_j}\{2K_j(\overline{M}_{m_j}^{-1} + \overline{M}_{s_j}^{-1})p_j\}r_{syn_j} \\ &\quad + 2\tau_{op_j}\overline{M}_{m_j}^{-1}p_j r_{syn_j} + 2\tau_{env_j}\overline{M}_{s_j}^{-1}p_j r_{syn_j} \\ &\quad + 2\tilde r_{sdj}K_j\overline{M}_{m_j}^{-1}p_j r_{syn_j} + 2\tilde r_{mdj}K_j\overline{M}_{s_j}^{-1}p_j r_{syn_j}.\end{aligned}$$

Using the property that $2\epsilon_1\epsilon_2 \le \gamma^2\epsilon_1^2 + \gamma^{-2}\epsilon_2^2$ where $\gamma > 0$, we have

$$\begin{aligned}\dot V_j \le &-r_{syn_j} N r_{syn_j} - r_{syn_j} r_{syn_j} \qquad (28) \\ &+ \gamma_{op_j}^2|\tau_{op_j}|^2 + \gamma_{env_j}^2|\tau_{env_j}|^2 + \gamma_{m_j}^2|\tilde r_{md_j}|^2 + \gamma_{s_j}^2|\tilde r_{sd_j}|^2\end{aligned}$$

where, N is defined as follows

$$\begin{aligned}N = &2K_j(\overline{M}_{m_j}^{-1} + \overline{M}_{s_j}^{-1})p_j - \gamma_{op_j}^{-2}p_j^2\overline{M}_{m_j}^{-2} - \gamma_{env_j}^{-2}p_j^2\overline{M}_{s_j}^{-2} \\ &-\gamma_{m_j}^{-2}p_j^2\overline{M}_{m_j}^{-2}K_j^2 - \gamma_{s_j}^{-2}p_j^2\overline{M}_{s_j}^{-2}K_j^2 - 1. \qquad (29)\end{aligned}$$

If the LMI (26) holds, then $N > 0$. Using *Assumption 2*, *Lemma 2* and the fact that $r_{syn_j}^2 = V_j/p_j$, following differential inequality is obtained

$$\dot V_j \le -\frac{V_j}{p_j} + \gamma_{op_j}^2 c_{op_j}^2 + \gamma_{env_j}^2 c_{env_j}^2 + \gamma_{m_j}^2 c_{m_j}^2 + \gamma_{s_j}^2 c_{s_j}^2.$$

The solution of this differential inequality is given as follows

$$V_j(t) \le V_j(0)e^{-\frac{t}{p_j}} + p_j C_j\{1 - e^{-\frac{t}{p_j}}\} \qquad (30)$$

where $C_j = \gamma_{op_j}^2 c_{op_j}^2 + \gamma_{env_j}^2 c_{env_j}^2 + \gamma_{m_j}^2 c_{m_j}^2 + \gamma_{s_j}^2 c_{s_j}^2$. Using the assumption that $\boldsymbol{r_{syn}}(0) = 0$, we have $V_j \le p_j C_j$. Therefore, $|r_{syn_j}| \le \sqrt{C_j}$ is obtained. Let q_{md_j}, q_{sd_j} be j-th element of the vector $\boldsymbol{q_{md}}, \boldsymbol{q_{sd}}$, then, we have following equation from definition of r_{syn_j}

$$r_{syn_j} = \dot q_{md_j} - \dot q_{sd_j} + \lambda_j(q_{md_j} - q_{sd_j}).$$

From this equation, $q_{md_j} - q_{sd_j}$ can be expressed as

$$q_{md_j} - q_{sd_j} = e^{-\lambda_j t}\{q_{md_j}(0) - q_{sd_j}(0)\} + \int_0^t e^{-\lambda_j(t-t')}r_{syn_j}dt'.$$

This equation and the fact that $|r_{syn_j}| \le \sqrt{C_j}$ give

$$|q_{md_j} - q_{sd_j}| \le |e^{-\lambda_j t}\{q_{md_j}(0) - q_{sd_j}(0)\}| + \sqrt{C_j}\int_0^t e^{-\lambda_j(t-t')}dt'.$$

Hence, we have

$$\lim_{t\to\infty}|q_{md_j} - q_{sd_j}| = \sqrt{C_j}/\lambda_j. \qquad (31)$$

Furthermore, definition of $\boldsymbol{r}_{syn}$ gives following inequality

$$|\dot q_{md_j} - \dot q_{sd_j}| \le \lambda_j|q_{md_j} - q_{sd_j}| + |r_{syn_j}|.$$

Therefore, we have

$$\lim_{t\to\infty}|\dot q_{md_j} - \dot q_{sd_j}| \le 2\sqrt{C_j}. \qquad (32)$$

Using the equations (27)(31)(32), we obtain

$$\lim_{t\to\infty}|q_{m_j} - q_{s_j}| \le \sqrt{C_j}/\lambda_j, \quad \lim_{t\to\infty}|\dot q_{m_j} - \dot q_{s_j}| \le 2\sqrt{C_j}.$$

(proof of 2)):If $\boldsymbol{\tau_{op}}, \boldsymbol{\tau_{env}} = 0$, prediction errors are also zero. Therefore, error system dynamics become $\dot{\boldsymbol{r}}_{\boldsymbol{syn}} = -(\overline{\boldsymbol{M}}_{\boldsymbol{m}}^{-1} + \overline{\boldsymbol{M}}_s^{-1})\boldsymbol{K}\boldsymbol{r_{syn}}$. It is easy to prove the lemma by using the fact that this system is asymptotically stable. ■